Chapter

Low-Frequency Electromagnetic Signals Observed before Strong Earthquakes

Igor I. Rokityansky, Valeriia I. Babak and Artem V. Tereshyn

Abstract

We consider two kinds of signals preceding earthquake (EQ): intensification of internal electromagnetic (EM) field – lithosphere emission (LE) and change of the Earth interior response function (RF). Several cases of LE before strong EQs were reviewed and analyzed, and preliminary portrait of LE precursor was compiled. LE can appear several times with lead time month(s), weeks, days, and hours and can attain amplitude of several hundreds of nT which not uniformly decreases with increasing distance from the source. Typical LE frequency content/maximum is 0.01–0.5 Hz. Data of 19 Japanese geomagnetic observatories for 20 years preceding the Tohoku EQ on March 11, 2011 were analyzed, and RFs (mainly induction vector) were calculated. At six observatories in 2008–2010, anomalous variations of RF were separated which can be identified as middle-term precursors. Applying the original method developed in Ukraine, a short-term two-month-long precursor of bay-like form was separated by phase data of observatory KNZ in the Boso peninsula where electrical conductivity anomaly was also discovered. Hypothetical explanation based on tectonic data is advanced: Boso anomaly connects two large-scale conductors—Pacific seawater and deep magma reservoir beneath a volcanic belt. Between two so different conductors, an unstable transition zone sensitive to changes of stress before strong EQs can be expected.

Keywords: geomagnetic field, lithosphere emission, conductivity structure, induction vector, earthquake precursor

1. Introduction

One of the long lasting challenges for the Earth sciences is earthquake (EQ) prediction. EQ precursors deliver unique information which is necessary for the solution of two interconnected fundamental problems—EQ prediction (humanitarian practical aspect) and support to the development of EQ theory (scientific aspect).

The history of the EQ precursor study goes back to antiquity. But even now their study remains purely empirical, and any precursor even recorded with perfect instrument can be treated as not related with seismicity (skepticism to prediction widely spread now), and it is difficult to prove that it is genuine EQ precursor because physics of EQ preparation process is still not well understood. The causes of such situation are (1) the complexity of the real Earth and processes

in it, (2) the absence of direct information from the place of EQ preparation, nucleation, and occurrence in the Earth interior. Nevertheless, consider the unique case of the successful EQ prediction—Haicheng prediction.

1.1 Haicheng EQM7.3

The Haicheng EQM7.3 occurred on February 4, 1975 at 19:35 local time in northeast China. After 1965, activation of seismicity occurred in an area of 120 km to SSW from Beijing with several destructive EQsM > 6. After this *long-term prediction*, the Chinese government greatly strengthened EQ study and precursor monitoring (telluric currents, well water, animal behavior, and other phenomena related with EQ) attaching to observation experts and also amateurs and scholars. Many precursors were observed in 1973 and 1974 in a large area of 200 × 300 km (*middle-term precursors*) which in December 1974–January 1975 concentrated in a smaller area. In January 1975, quiescence of seismicity was observed but anomalies of groundwater, telluric currents, radon, tilt, animal behavior, etc. increased till January 23 (*short-term precursors*), then slightly decreased, and since February 1 rouse in hundreds times. From 16:00, February 3, to 18:30, February 4, 500 EQs with M up to 4.2 occurred in the area between Yingkou and Haicheng cities. They were interpreted as foreshocks of strong EQ. Emergency evacuation was ordered by authorities, and law-abiding Chinese left their houses. At 19:36, a devastating EQ struck dozens of cities including Haicheng with almost 1 million inhabitants. Thousands of buildings collapsed, but hundred thousand lives have been saved by the well-timed prediction. Instructive lessons from successful Haicheng prediction are (1) continuous transition from long–/intermediate-term prediction to short/immediate ones with consistent improvement of expected EQ time, place, and magnitude; (2) close cooperation of authorities, scientists, amateurs, and mass media; and (3) the use of all available precursors, including "nonscientific" ones as animal behavior [1].

Multiparameter monitoring and strong scientific efforts of the last decades reveal some unexpected features of precursors: (1) Long-distance appearance up to thousands km from EQ epicenter. (2) Spatial selectivity: EQ precursors can be observed in some sensitive zones (usually fault zones) and be not observable in vast territories even not far from impending EQ. (3) Spatial–temporal migration of precursors: initially it appears in one locality, and then it appears in the next locality, usually with changed parameters. Such features did not find explanation in the framework of simple dominant ideas in the middle of the twentieth century about geological media. These features evidenced the complexity of geological media, and in the second half of the twentieth century, several new concepts have appeared to explain new data (Sadovsky MA, Varotsos P, Gufeld IL and many others).

For effective EQ prediction, we need automatic system of monitoring, processing, and analysis of all observed precursory parameters, their cross-correlation analysis to estimate probability of expected EQ (taking into account all previous global, regional, and local analyzes). High-level scientific team must keep contact with decision-making authorities for providing public announcement of the EQ prediction and plan of emergency measures. Such system needs great funds. Some elements of such system are created in few regions (California, China, ex-USSR countries).

1.2 Goal and scope of the chapter

Multitude of EQ precursors is the unique base for EQ prediction. Complexity of the earth and poor understanding of seismicity process enforce us to use as many

kinds of precursors as possible. Two approaches are perspective for the fishing of the precursory signals from geomagnetic data: (1) Direct observation of the lithosphere emission (LE) of the internal electromagnetic fields arising in the course of EQ preparation and nucleation process and (2) transformation of the time series of the observed three components of geomagnetic field into time series of response functions of the Earth's interior conductivity.

In the next sub-section, we review few case stories of the most reliable records of ultralow-frequency (ULF) LE.

In Section 2, we shortly outline the rather sophisticated methodology of response function (RF) approach referring for details to few monographs [2–5].

In Sections 3 and 4, we apply RF method to the Japanese geomagnetic observatories data in the attempt to separate the precursors of great Tohoku EQM9 11.03.2011, wherein obtained quite reliable result on the Boso conductivity anomaly and advance its tectonic interpretation.

In Section 5, we discuss the results obtained.

In Section 6, we summarize the results and give the recommendations for the improvement of the low-frequency EM precursor study.

1.3 Case stories of LE records before strong EQs

There are many reports on LE registration, in particular before EQs. Consider fortunate cases when EM observations turned out to be located in the places where LE field was well above magnetotelluric (MT) field+noise background and can be easily identified.

1.3.1 Great Alaska EQM9.2 on March 28, 1964

Geomagnetic observatory in the city of Kodiak was located in the distance of 440 km from the epicenter of the EQ and only in 30 km from the fault zone along which displacement occurred. The full field proton magnetometer recorded several magnetic disturbances. The strongest one with intensity 100nT appeared 1 h 06 min before the EQ [6].

1.3.2 Loma Prieta EQM7.1 on October 18, 1989

One of the most convincing cases of LE precursors was recorded before that EQ [7]. The monitoring system of Stanford University (created for traffic noise study) operated since October 1987 at the distance of 7 km from the future EQ epicenter. The system included induction coils and special computer which calculated half-hourly averages of the magnetic field power spectra in each of nine narrow frequency bands covering the overall range 0.01–10 Hz.

During 23 months record was normal with low noise. After September 12, 1989, anomalous signal began to appear in two frequency bands: 0.05–0.1 and 0.1–0.2 Hz and grew up to 1.5 nT. In October 5, a large increase of amplitude appeared at all frequencies with the strongest one at the lowest frequency 0.01 Hz, where it reached 30 times the normal level. On the last several days before EQ, anomaly gradually diminishes (a quiescence!), and 3 h before the EQ, very large amplitude appeared only at periods longer 0.5 Hz, exceptionally large at frequency 0.01 Hz. We must emphasize that instrumentation of Stanford University which allowed to get results every half an hour is very good for LE monitoring. Unfortunately, it did not continue the operation for EQ prediction.

1.3.3 Caucasus

Kopytenko et al. [8, 9] developed three-component magnetometers for frequency range 0.005–10 Hz. The first instrument started the record 23 days before destroying Spitak EQM6.9 at 7.41 UT, on December 7, 1988, in geomagnetic observatory at Dusheti, 129 km to the north from the EQ epicenter. It recorded intensive $\mathbf{B}_{LE}$ which started 4 h prior the EQ (**Figure 1a**, **b**).

In the time interval November 14, 1988 to March 5, 1989 in frequency range 0.1–1 Hz 59 unusual noise-like bursts of LE with an amplitude well higher the background noise (0.03 nT) and the duration ranging from several minutes to several hours (mean duration ≈30 min) were recorded mainly before the strong aftershocks. Decrease in aftershock activities and $\mathbf{B}_{LE}$ activity was quite synchronous.

The next strong event was Racha EQM6.9 at 9.13 UT, on April 29, 1991, occurred at the epicentral distance of 90 km from Dusheti where no pronounced $\mathbf{B}_{LE}$ were recorded. It means that Dusheti is not a sensitive place for the EQs in Racha region (effect of spatial selectivity). Kopytenko's team organized $\mathbf{B}_{LE}$ observations in two field sites Nik and Oni for June–July 1991—the time of Racha aftershock activities. Forty-seven $\mathbf{B}_{LE}$ with intensity up to 2 nT and duration ranging from several minutes to several hours were observed at both observatories, 23 of them were recorded 1–4 days before the strong aftershock M6.2 on June 15,1991. **Figure 1c** presents $\mathbf{B}_{LE}$ bursts observed before aftershock M4.0. The distance from the epicenter to Oni was two times smaller than to Nik, but intensity of LE signal at Nik was considerably larger: for H component in 10–20 times, for D in 1.3–2 times, and for Z in 5–7 times. It means strong spatial selectivity of the LE signals preceding EQ [10, 11].

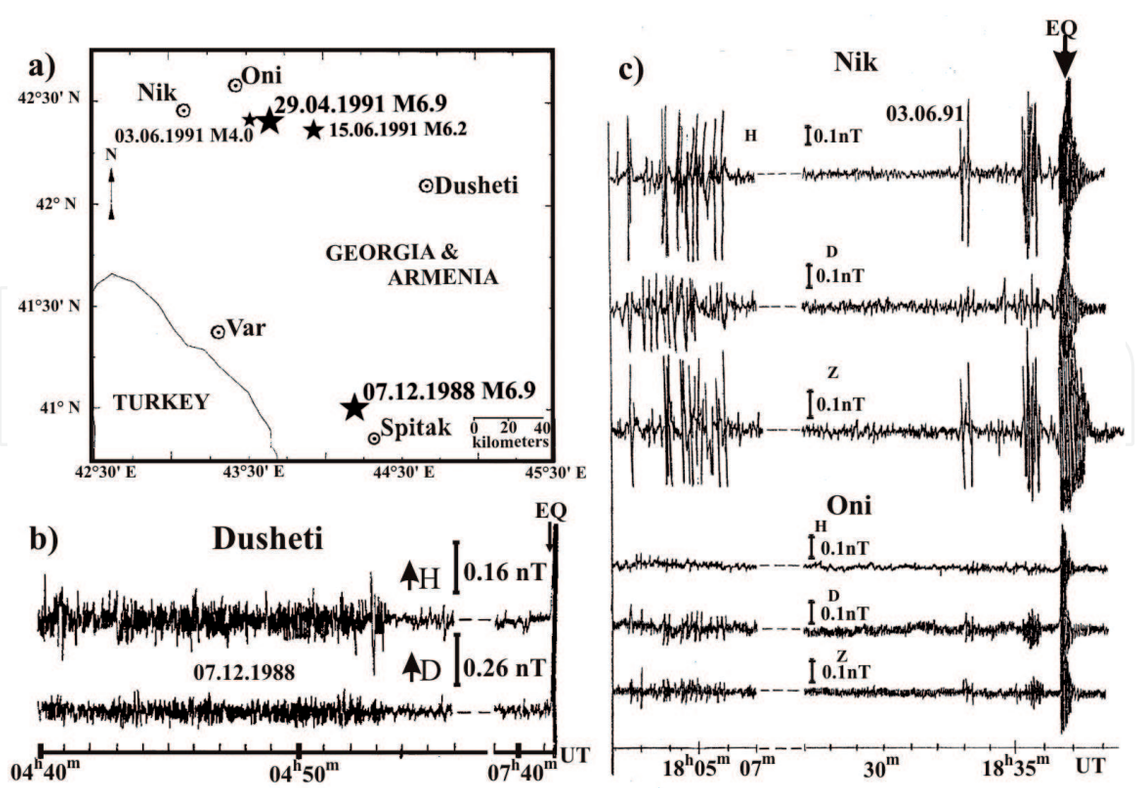

Figure 1.
$\mathbf{B}_{LE}$ preceded some EQs in Caucasus [8, 9]. (a) Map of seismoactive region with the sites of observation and epicenters (given by stars) of the events discussed in text. (b) Final fragment of $\mathbf{B}_{LE}$ record started 4 h before Spitak EQ and abruptly terminated 2 h 48 min before it. (c) Several short $\mathbf{B}_{LE}$ bursts records during 33 min before aftershock M4.0 at field stations Nik and Oni located at the distance 34.6 and 16.9 km from the epicenter correspondingly.

In the conclusion we like to emphasize that magnetometers in described studies can register variations in the frequency band of 0.005–10 Hz, but they recorded most intensive $\mathbf{B}_{LE}$ at the frequencies 0.1–1 Hz that differs from the result in Loma Prieta, where the maximum tends to their lowest frequency 0.01 Hz.

1.3.4 Taiwan

The island-wide geomagnetic network consisted of three-component geomagnetic observatory LP in the seismically quiet area and seven full field stations equipped by proton magnetometers with 0.1 nT sensitivity and sampling rate of 10 min distributed in areas of high seismicity [12]. Chi-Chi EQM7.6 occurred on September 21, 1999, in the middle of Taiwan. Stations LY turned out to be just near to surface rupture of the EQ along Chelungpu fault and recorded the strongest LE which clearly separated from comparison with records of remote observatory LP. LE begun more than a month before the EQ and attained in maximum 200 nT, and then its amplitudes gradually weakened, and the disturbance level reduced to that of a quiet period almost right after the second strong Chia-Yi EQM6.4 that occurred near the southern end of the Chelungpu fault on October 22, 1999 [12].

1.3.5 Greece

In Greece in the early 1980s for the registration of the LE electric components, the so-called seismic electric signals (SES) special network was created by Prof.

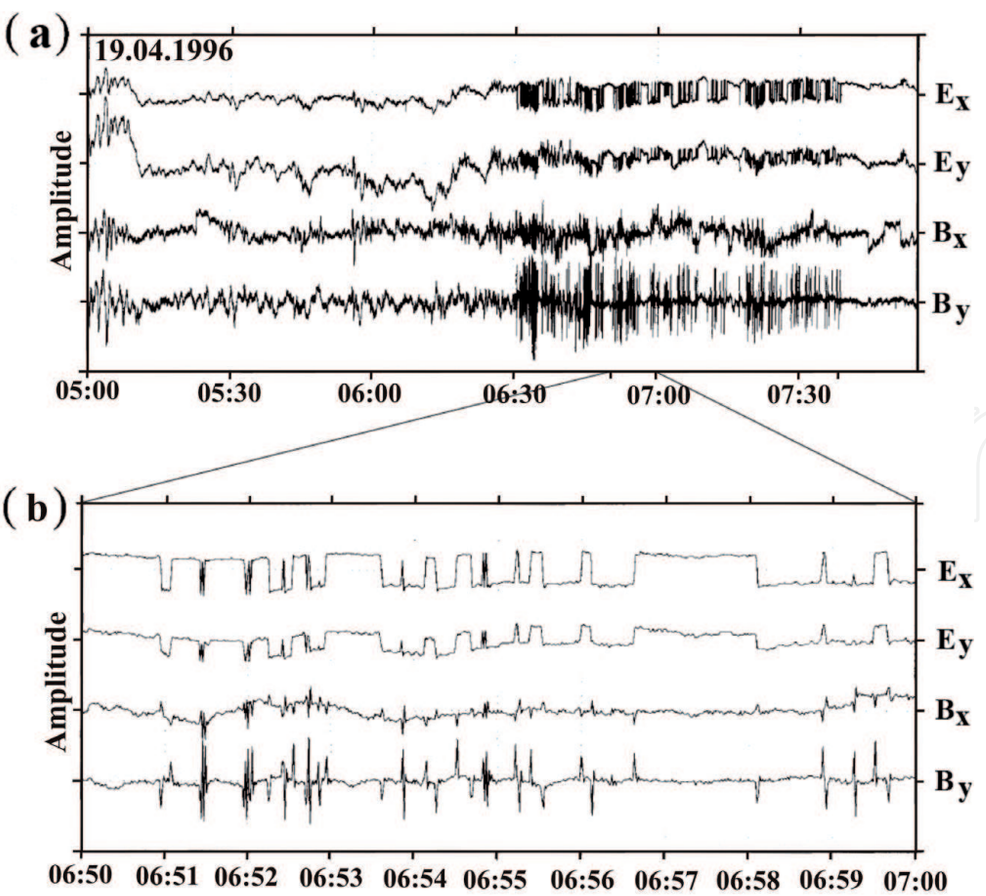

Figure 2.
The SES activity on April 19, 1995, before the Grevena-Kozani EQM6.6 on May 13, 1995, recorded in Greece at the IOA observatory at the distance of 80 km from the epicenter with a sampling rate of 1 sample/s: (a) 3 h record with strong SES activity in 6.30–7.40 time interval, (b) is the 5 min fragment of (a), showing both electric and magnetic components in expanded time scale [11]. Amplitudes are given in relative units.

P. Varotsos [11, 13]. The network consists of 10–15 stations. Each station included several (from 6 up to 100) grounded electrical dipoles with the length from 50 m up to 20 km that allows to study spatial characteristics of observed field and separate SES from MT field and noise. In the course of continuous monitoring for more than 35 years, Prof. Varotsos and collaborators identified (as the result of a posteriori analysis) many SES before the following EQs and studied their regularities [11], for example, the selectivity effect: SES can be observed in some sensitive zones and be not observable in vast territories even not far from impending EQ. Prof. Varotsos made a number of correct EQ predictions registered officially before the event. We show interesting case of joint registration SES and horizontal magnetic components recorded on April 19, 1995, 25 days before Grevena-Kozani EQM6.6 on May 13, 1995 (**Figure 2**). Magnetic components look as derivative of electrical impulses that are clearly seen in the lower graph (b) with expanded time scale. In the latter years, Prof. Varotsos' group develops deeper insight in the physics of LE: entropy and natural time analysis for the better understanding of the EQ preparation process and for the distinguishing LE signals from similarly looking variations of MT and noise origin [14, 15].

2. Basic concepts and definitions. Methodology

2.1 Varying geomagnetic field

Varying geomagnetic field $\mathbf{B}(t) = B_x\mathbf{e_x} + B_y\mathbf{e_y} + B_z\mathbf{e_z}$ (where $\mathbf{e_x}$, $\mathbf{e_y}$, and $\mathbf{e_z}$ are unit vectors directed to north, east, and downward correspondingly) continuously exists in and around the Earth and is recorded nowadays digitally with a time reading interval Δt (1 min or 1 s in our study). All components are functions of time t which we skip out for brevity.

2.2 Main sources of observed geomagnetic field

$$\mathbf{B}(t) = \mathbf{B}_{MT} + \mathbf{B}_{noise} + \mathbf{B}_{LE}, \quad (1)$$

where $\mathbf{B}_{MT} = \mathbf{B}_{MT}ext + \mathbf{B}_{MT}intn + \mathbf{B}_{MT}inta$ is the magnetotelluric field.

$\mathbf{B}_{MT}ext$ is the external primary magnetic field of the currents in magnetosphere and ionosphere of the Earth.

$\mathbf{B}_{MT}intn$ is the normal internal secondary magnetic field of the currents induced by $\mathbf{B}_{MT}ext$ in the Earth's interior having a hypothetical "normal" horizontally layered conductivity structure. The horizontal components of $\mathbf{B}_{MT}intn$ add together with $\mathbf{B}_{MT}ext$ increasing observed horizontal MT-field up to doubling over hypothetical ideally conducting Earth. On the contrary, the vertical component of $\mathbf{B}_{MT}intn$ subtracts from $\mathbf{B}_{MT}ext$ diminishing observed normal vertical MT field up to 0 (phase neglected).

Thus, $\mathbf{B}_{MT}n = \mathbf{B}_{MT}ext + \mathbf{B}_{MT}intn$ has the horizontal component much greater than the vertical one and embraces great territory equal to external source field dimension.

$\mathbf{B}_{MT}inta$ is the anomalous internal secondary field arising on local/regional conductivity anomalies as a result of redistribution of the currents responsible for $\mathbf{B}_{MT}intn$.

Such subdividing of secondary internal field is rather artificial, but it is used in geoelectromagnetic methods: $\mathbf{B}_{MT}intn$ in sounding methods, magnetotelluric sounding (MTS) and geomagnetic deep sounding (GDS); $\mathbf{B}_{MT}inta$ in profiling one, magnetic variation profiling (MVP) [2–5].

Bnoise is the ever-present noise, both man-made and natural.

$\mathbf{B_{LE}}$ is the purely internal field of lithosphere emission, it is usually local and transient, and the ratio of vertical component to the horizontal one usually differs from the same ratio for MT field.

After the conventional processing using Fourier transform, a $\mathbf{B}(t)$ record of duration $t_2–t_1$ is transformed into a superposition of harmonic components with periods $T_1, T_2...T_n$.

2.3 Response function

Response function is the term widely used in natural sciences and mathematics. In the geoelectromagnetic studies of *electrical conductivity* σ (x, y, z) of the Earth's interior [2–4], the RFs are supposed to be some functions derived from the Earth's electromagnetic (EM) data that provides us with a possibility to determine the conductivity structure of the Earth. EM RFs are usually frequency/(period T) dependent, and then they are complex functions having real (index u) and imaginary (index v) parts. We use two of these functions.

2.3.1 Induction vector

Induction vector $C = A\mathbf{e_x} + B\mathbf{e_y}$ (A and B are determined from the linear equation: $B_z = AB_x + BB_y$). Real induction vectors $\mathbf{C_u} = A_u\mathbf{e_x} + B_u\mathbf{e_y}$ possess an important property: in the notation of Wiese used here, they are directed away from a good conductor.

2.3.2 Anomalous horizontal magnetic variation tensor

Anomalous horizontal magnetic variation tensor [M] is determined from the linear system of equations $B_x(\mathbf{r_i}) = M_{xx}B_x(\mathbf{r_0}) + M_{xy}B_y(\mathbf{r_0})$ and $B_y(\mathbf{r_i}) = M_{yx}B_x(\mathbf{r_0}) + M_{yy}B_y(\mathbf{r_0})$, where $\mathbf{r_0}$ and $\mathbf{r_i}$ are coordinates of base (reference) and some other observation place. Tensor [M] reflects the change in geoelectric structures between two places (if the source field used is uniform).

2.4 The processing of observed geomagnetic field

The processing of observed geomagnetic field $\mathbf{B}(t)$ for the monitoring of geodynamic and other environmental processes implies transformation of three components of geomagnetic field time series with time reading interval Δt (1 min or 1 s in our study) into a variety of time series with temporal resolution $\Delta\tau$ ($\Delta\tau \gg \Delta t$) of different RF components: *Re* and *Im* and *x* and *y* at the set of periods $T_1, T_2...T_n$ of received harmonics ($\Delta t \ll T_i \ll \Delta\tau$).

2.5 The theory of geoelectromagnetic methods

The theory of geoelectromagnetic methods [2–4] is developed for natural source field in the form of vertically incident plane wave (Tikhonov-Cagniard (T-C) model), which usually holds for an external source field of magnetosphere-ionosphere origin (named as magnetotelluric field) for the periods less than 10^4 s. Ideally RF depends only on the Earth's conductivity distribution which is sensitive to the stress variations and therefore to geodynamic processes including the earthquake preparation.

3. Variations of geomagnetic response functions (mainly induction vector) before the 2011 Tohoku earthquake

RFs and their variations, especially in relation with EQs preparation, were studied in Japan for many years and were described in many works among which we cite only few [16–18]. In the last two decades, the RF approach became less used for EQ studies because of strong noise at Japanese observatories. After the catastrophic Tohoku EQ on March 11, 2011, near Japan, we analyzed the available geomagnetic data to obtain some EQ precursors using the RF method. Some results were presented in Russian [19–21], which together with the latest results of our study will be summarized below.

Data used: We obtained data of 17 Japanese geomagnetic observatories (**Figure 3**, **Table 1**) for time interval of 12–20 years with temporal reading every 1 min (and few observatories with 1 s reading). For the conversion of geomagnetic field **B** time series into RF time series, we used the advanced multi-window remote reference (rr) robust programs with coherency control [22, 23]. After processing we got values of four components of induction vector A_u, B_u, A_v, B_v for each day for five period intervals centered at: 225, 450, 900, 1800, and 3600 s. To reduce the great scattering, everyday values were smoothed with moving windows and/or were found average or median values for some interval (usually 1 month).

3.1 Results of processing for separation of middle-term precursors

Analyzing large material of processed data for 15 years from 2001 till 2015, we found that aperiodic variations (or enhancement of annual variation) of induction vectors were observed at periods 225, 450, and 900 s during 3–5 years before the Tohoku EQ at stations: HAR, KAK, OTA, KNZ, and TTK, most clearly at period 450 s presented in **Figure 4**. We should emphasize that no such aperiodic variations were observed at other stations including ESA and MIZ, which are the nearest to the EQ epicenter. The best correlation of middle-term anomalies is observed between the two most remote (620 km) from each other stations HAR and TTK: at both we see strong synchronous variations of induction vectors with maxima in the end of 2008, the end of 2009, with several maxima in 2010, in the beginning of 2011, and

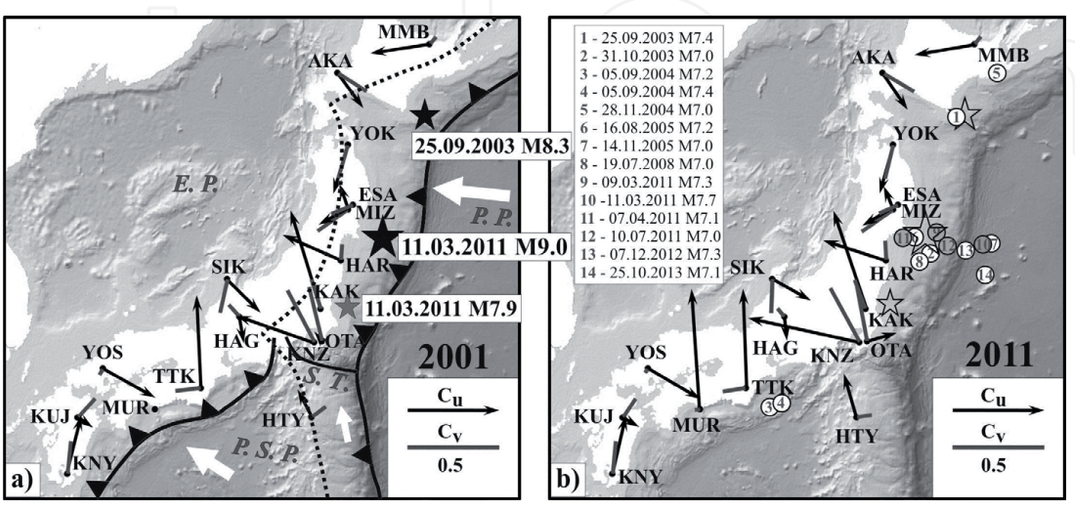

Figure 3.
Map of Japan with real $\mathbf{C}_u$ and imaginary $\mathbf{C}_v$ induction vectors for the period 450 s at 17 geomagnetic observatories by 1 min record data. (a) Mean vectors for the year 2001. Stars present EQs with M > 7.8 since 2001. Elements of plate tectonics; white arrows represent the directions of plate motions; E. P., Eurasian plate; P. P., Pacific plate; P. S. P., Philippine Sea plate; S. T., Sagami trough; dotted line, volcanic front. (b) Mean vectors for 2011. Circles present EQs with M ≥ 7. The depth of hypocenters is less than 50 km for all EQs.

Code	Station name	Geom. lat.	Geom. long.	Geogr. lat.	Geogr. long.	Processed years
MMB	Memambetsu	35.44	148.24	43.910	144.189	1993–2012
AKA	Akaigawa	34.31	151.09	43.072	140.815	2001–2012
YOK	Yokohama	32.28	150.43	40.993	141.240	2001–2012
ESA	Esashi	30.55	150.09	39.237	141.355	1997–2012
MIZ	Mizusawa	30.41	150.21	39.112	141.204	1997–2015
HAR	Haramachi	28.90	150.25	37.615	140.953	2001–2015
SIK	Shika	28.04	153.96	37.082	136.773	2001–2012
KAK	Kakioka	27.47	150.78	36.232	140.186	1956–2015
HAG	Hagiwara	26.98	153.47	35.985	137.186	2001–2012
OTA	Otaki	26.54	150.63	35.292	140.230	2001–2015
KNZ	Kanozan	26.48	150.87	35.256	139.956	1996–2016
YOS	Yoshiwa	25.12	157.87	34.476	132.176	2001–2012
TTK	Totsukawa	24.83	154.52	33.932	135.802	2001–2015
HTY	Hatizyo	24.30	150.75	33.073	139.825	1991–2008
MUR	Muroto	24.10	155.99	33.319	134.122	2004–2012
KUJ	Kuju	23.65	158.58	33.061	131.260	2001–2015
KNY	Kanoya	22.00	158.80	31.424	130.88	1991–2016

Table 1.
Geomagnetic observatories in Japan used in the study.

return to the previous level after the Tohoku EQ. We may suppose that these aperiodic variations can be the middle-term precursors of the Tohoku EQ. These observatories are located not at the shortest distance from the EQ, which is in agreement with well-known phenomenon of spatial selectivity of EQ precursors known during the centuries for hydrological precursors and recently proven for LE registered in the form of seismic electric signal [11, 13].

Having 1 min time series, we can analyze only geomagnetic variations with period T > 3 min, and the most interesting shorter part of ULF spectra (0.01–10 Hz), where strongest $\mathbf{B}_{LE}$ have been observed [7–9], is left not resolved. So, we get 1 s data for observatories KAK, KNZ, ESA, MIZ, and for short time intervals for UCU and KYS to analyze RF for periods T > 5 s.

3.2 Boso conductivity anomaly

Processing of records from 18 observatories (16 of them are shown in **Figure 3** and KYS and UCU in **Figure 5**) for the determination of horizontal tensors [M] with KAK as the base station yields the absence of noticeable horizontal tensor anomalies in ESA, MIZ, HAR, TTK, and MUR but reveals their existence in KNZ, UCU, OTA, and KYS (**Figure 4a**). In KNZ and OTA the enhancement of real tensor components M_{xx} and M_{yy} equals to ≈40% and ≈30% correspondingly at periods T < 500 s decreasing at longer periods. This result was supported by direct visual measurements described below. At closely located observatories KNZ and OTA, the latitudinal (E-W) component of induction vector at period 450 s and shorter increased (in 2011 comparatively to 2001) in opposite directions: westward in KNZ and eastward in OTA (see **Figure 3b**). It means that between these two observatories, an additional current (of geodynamic origin) appeared in 2011.

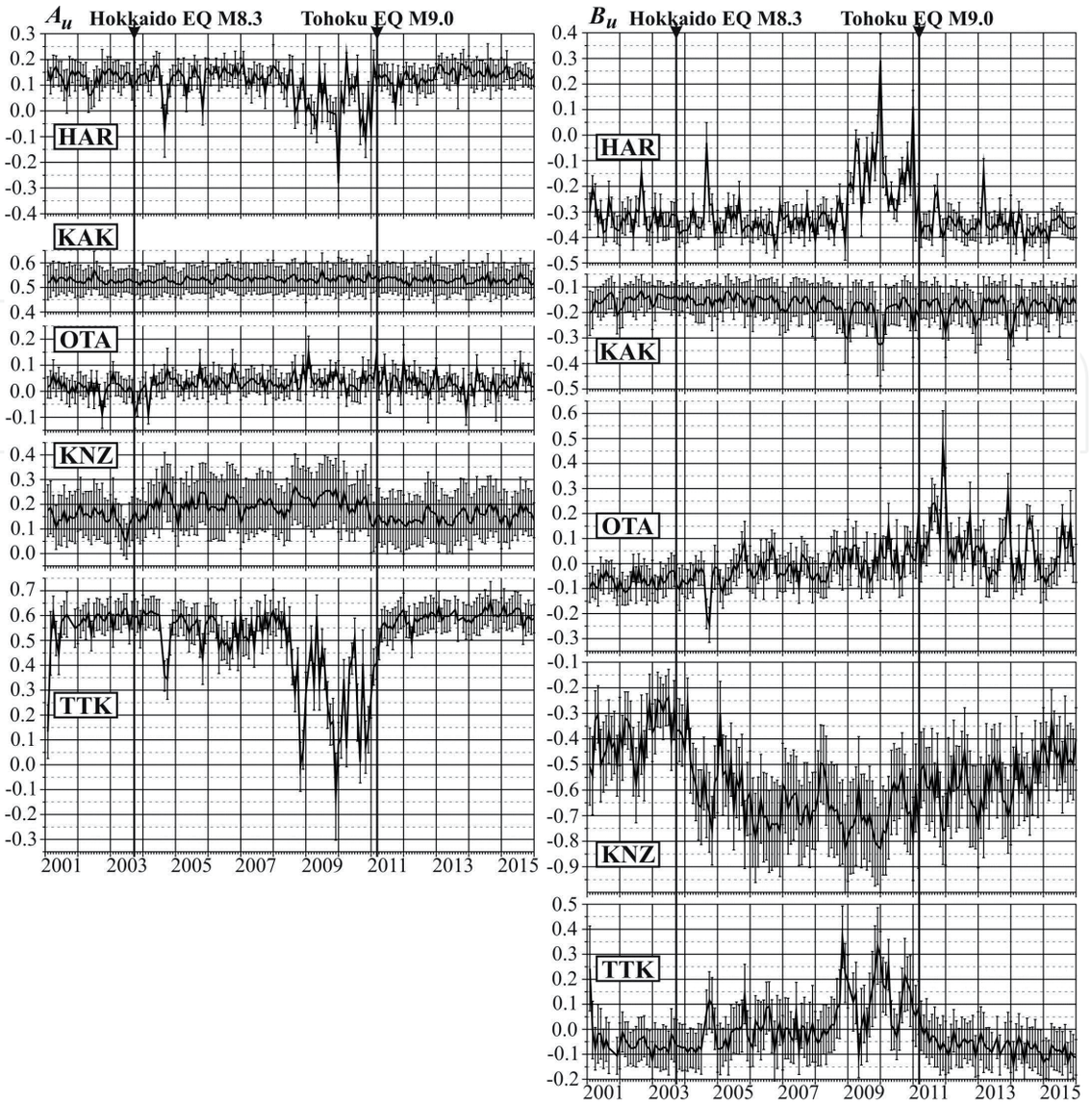

Figure 4.
Variations of the monthly mean induction vector components at the period of 450 s during 2001–2015 at five observatories with significant changes before the Tohoku EQ: HAR, KAK, OTA, KNZ, and TTK. Vertical bars present the uncertainty of every monthly mean value. Two strong EQs are shown by vertical lines.

3.2.1 Visual analysis of geomagnetic records

Considering the geomagnetic field synchronous records (**Figure 3a**), we noticed that magnetotelluric field appears synchronously at all observatories, while noise appears locally at each one. The stations most contaminated by noise are UCU and KNZ which are the nearest to DC railways. But during the after-midnight time interval from ≈1:30 to ≈4:30 LT (16:30–19:30 UT) the strong noise from DC railways almost disappears.

Direct measurements of the strong MT amplitude variations in each component provide a check (not precise but very reliable) of the results obtained by processing. So, the enhancement of B_x at KNZ and OTA at approximately 30–40% exists, and it can be interpreted only by the electrical conductivity anomaly under the observatories, i.e. under the central part of the Boso peninsula.

3.3 Comparison with geology and tectonic evidence

The relation between M_{xx} and M_{yy} anomalies in KNZ defines WNW-ESE strike of the Boso conductivity anomaly. Geological data [25, 26] presented in **Figure 4b–c**

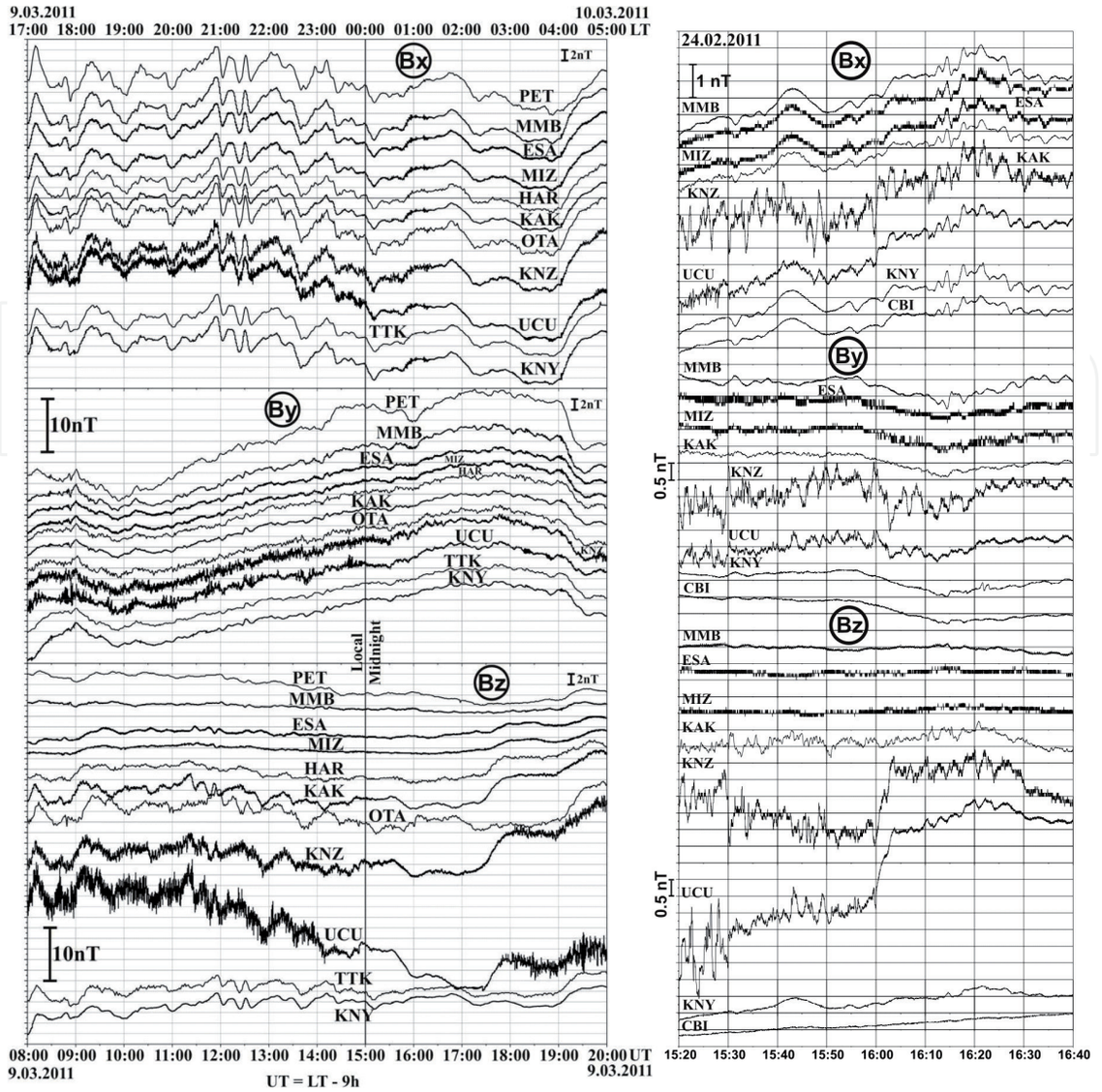

Figure 5.
(a) Synchronous records (1 min data) of 10 Japanese and 1 Kamchatka (PET) geomagnetic observatories 2 days before the Tohoku earthquake. In the UCU and KNZ observatories records, we see during daytime strong noise due to DC electric trains and an absence of this noise during the hours after midnight. Geomagnetic activity presented by global 3 h index Kp was as follows: in the 6–9 UT hours time interval Kp = 1+; in 9–12 UT hours, Kp = 1–; in 12–15 UT hours, Kp = 1; in 15–18 UT hours, Kp = 1–; in 18–21 UT hours, Kp = 1 + . (b) Synchronous record (February 24, 2011) (1 s data) of eight Japanese observatories 80 min after midnight (15 h UT). Magnetic activity was very low: Kp =0+. DC railway traffic is almost stopped, but the noise-like variations were not terminated in the Boso peninsula. Maybe it is a precursory LE which according to [24] started on February 22, 2011.

suggest the existence of anomalous conductor of WNW-ESE strike in Miura Group sediments of the Kanto plain at depth 0–4 km. Relations between M_{xx} and M_{yy} in UCU, OTA, and KYS are different as seen in **Figure 6a**. It means that the direction of anomalous currents is also different under each observatory. Calculations show that at least 50% of anomalous currents should be located near the surface in the sediments of the Kanto plain to fit the received data.

On the other hand, the plate tectonic evidences that the Boso anomaly is located over the Sagami trough, structure at the depth 15–20 km in the complex junction of three lithosphere plates (**Figure 3a**). Strike of the trough is the same, WNW-ESE, so some part of the anomalous conductor can be located in the Sagami trough.

The eastern part of both conductors (shallow sediments and deep trough) has contact with seawater, while the western one can contact with a magma reservoir. In such a circuit it can be some unstable area(s) with conductivity strongly dependent on stress and sensitive to stress changes related with EQs.

In **Figure 6b**, vectors are shown for a period of about an hour (4000 s), at which industrial noise is practically absent and vectors adequately reflect the heterogeneity of geoelectric structure. In **Figure 6c**, vectors at the period 25 s are built with dominated noise field, which is greater than MT field on four observatories considered. Real and imaginary vectors at periods 16, 25, 50, and partly at 200 s (**Figure 6d**) are directed to the source of noises—the nearest railway. To reduce influence of the noise, night records and remote reference technique were used (**Figure 6f**). Received corrected vectors appeared still very scattered (**Figure 6e**) and for monitoring of geodynamic processes can be used cautiously. However, vectors averaged over a long period of time can be used for clarifying of the geoelectric structure. Corrected real vector in KNZ at the shortest periods directs to north.

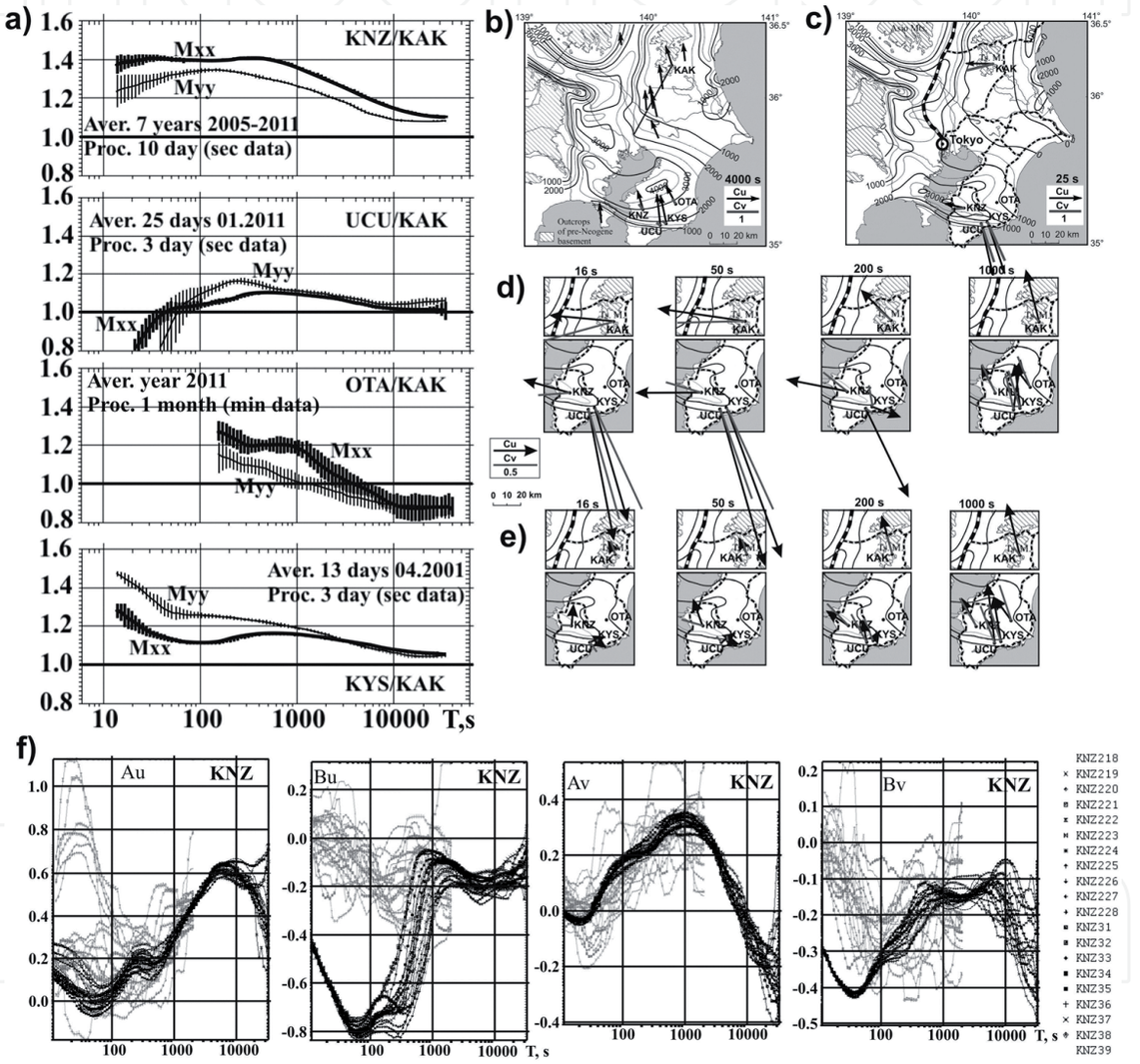

Figure 6.
RFs and Neogene sediments in the Kanto plain and the Boso peninsula. (a) Frequency characteristics of the modulus of horizontal tensor [M] main components at Boso observatories with reference to the base observatory KAK. Every curve is a mean value for 7 years (KNZ), 25 days (UCU), 1 year (OTA), and 12 days (KYS). Interval of averaging (aver.) with the date and the length of processed realizations (Proc.) is written at every graph (they were chosen depending on the interval of available data and their discreteness). (b) Thickness of Neogene sediments [25, 26] and induction vectors for period ≈1 h, named observatories with real and imaginary vectors—is our processing, the other six real vectors are taken from [16]. (c) Thickness of Miura group deposits with "N.8 half graben fills" and induction vectors for T = 25 s obtained from the dominant DC noise and directed to the noise source—DC railways given by thin lines for suburb railways and by thick line for magistral one. (d) Similar results for another four periods. (e) Results of the same data processing with an attempt to make away the impact of the noise by means of either only after-midnight 4 h use or by remote reference technique application. (f) Frequency characteristics of induction vector components at KNZ. Dark lines for the wide period range are the results of ss (single station) processing of 3-day realizations with sliding reference to middle day; light lines, processing of after-midnight 4 h records of the same 20 days from February 18 to March 9, 2011.

It means that the most conductive part of Boso electrical conductivity anomaly is located to south of KNZ, apparently near the southern side of the asymmetric "N.8 half graben fills" of the Miura Group sediments [26].

Results of the single station and nighttime records processing at KNZ are given in **Figure 6f**. We see that full-day and nighttime results significantly differ from each other only for B_u and partly B_v components because a railway is located to the west from KNZ and brings the distortions mainly in the eastern component. The northern component is less affected by noise at periods 100 s and more that opens the possibility to use it for separation of EQ precursor that will be used in the next section.

4. Short-term precursor separation

4.1 Introductory remarks

The induction vector derived from very noisy records, practically from noise field, has small stable phase. Therefore, if some other magnetic fields, which are usually not so stable (let it be a precursor field), are superimposed on the field of noise, exactly the phase of induction vector will be the most sensitive component for a precursor separation.

Below we apply a new approach developed by Tregubenko [27], who used it for processing the data of seismo-prognosis monitoring network in Ukraine. He separated precursors before few strongest ($M \approx 4$) Crimean EQs occurred during 15 years, in particular before the Sudak, Crimea EQM3.9 on January 24, 2005 [27]. We applied this approach to KNZ, KAK, and ESA 1-s data, but the precursor was found only in KNZ. We can explain this by the spatial selectivity of the precursors: high sensitivity of KNZ place is quite natural in virtue of Boso electrical conductivity anomaly located just under KNZ observatory.

4.2 Processing of KNZ data

The processing was made with the use of Varentsov's [22] program. Coherences were used as weight estimates for averaging the results. To minimize the effect of noise, the estimates with multiple coherences less than 0.7 were ignored that allowed us to obtain minimally shifted estimates of induction vector's components. Maximum anomalous effect before the Tohoku EQ was observed for the phase of the induction vector northern component—$\arg(A)$ for periods 100–200 s. For the longer periods, the anomaly gradually decreases, so that we now present the results for T = 100 s. The processing and analysis were made in two steps:

Step 1. A 7-year-long (2005–2011) geomagnetic field time series with every 1 s reading was processed for every month as a single unit. $\mathrm{Arg}(A)$ time series with every month reading were received as in **Figure 7a** and analyzed by a polynomial approximation approach. The most significant first-, second-, and seventh (quasi-annual)-order polynomials were extracted from the rough data, and we obtained **Figure 7b** which is more perspective for comparison with EQs. But 1-month temporal resolution of RF is not sufficient for such an analysis. As for the Tohoku EQ precursors, we see a 9-month-long negative anomaly in 2010 approximately 1 year before the main event.

Step 2. A 2-year-long (2010–2011) 1 s time series were processed for every day as single unit. Large scatter of everyday results was reduced by averaging with moving window of 5 days long with 1-day shift. From these curves, i.e., $\arg(A)$ time series with everyday reading, we extracted first-, second-, and seventh (quasi-annual)-order polynomials determined in step 1. The result is shown by the gray rough curve

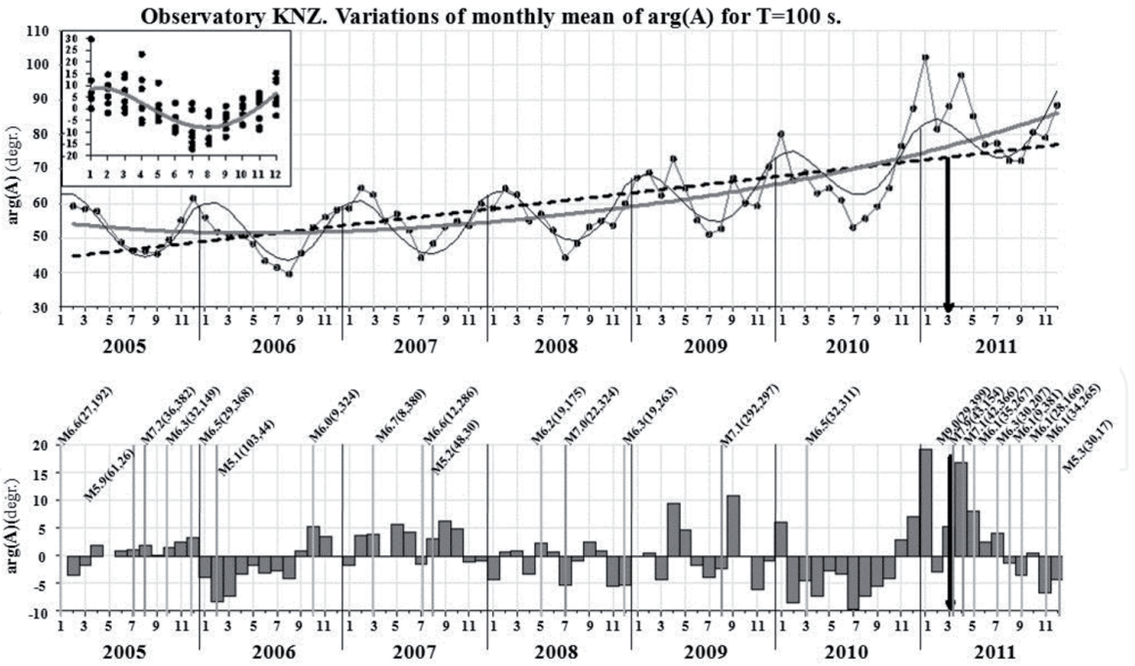

Figure 7.
*Variations of arg(*A*) for the period T = 100 s at the observatory KNZ during 2005–2011. (a) Monthly values of arg(*A*) are given by dots. The dashed straight line and bold solid line are the first- and second-order polynomials, respectively. Thin smooth line is quasi-annual variations obtained as seventh-order polynomial approximation. In the upper left corner, the determination of mean annual variation is shown (first- and second-order polynomials were excluded). (b) Variations of arg(*A*) after removal of the first-, second-, and seventh (quasi-annual)-order polynomials. Moments of strong EQsM > 5 are indicated by vertical lines with given magnitude M (the first number in parentheses is the depth of the hypocenter, and the second one is distance from epicenters to the observatory KNZ, both are given in km).*

in **Figure 8a**. The bold solid line is the result of averaging with moving window of 29 days with 1-day shift to suppress monthly variations arising from the Moon rotation around the Earth (gravity effect) and the Sun rotation around its axis (magnetic activity effect). The mean for 7 years 2005–2011 annual variation have been subtracted, but we see a residual annual variation in **Figure 8a** (RF annual variation enhancement was recorded at several observatories 2–3 years before Tohoku EQ and can be considered as middle-term precursor). So, such a residual annual variation was determined once more from 2-year data presented in **Figure 8a** and subtracted; the result is presented in **Figure 8b**.

4.3 Discussion of short term precursor

The variations of arg(*A*) given by the bold solid line in **Figure 8b** are cleaned from periodic variations of annual and monthly periods, which make it more convenient to identify EQ precursors. Indeed, we see a strong bay-like variation that begins almost 2 months before the Tohoku EQ and has approximately 2-month duration. This is in good agreement with the finding of Prof. Varotsos' team [14, 15]. In particular, Varotsos et al. showed that the initiation of an SES activity in Japan appears almost simultaneously with the minimum of the fluctuations of the order parameter of seismicity analyzed in natural time, and such a minimum was clearly observed [15] on January 5, 2011, that is, almost 2 months before the Tohoku EQ occurrence.

Time of beginning of a bay-like precursory variation and its duration depends on the magnitude of an expected EQ. This time is equal to approximately 2 weeks for the processed Crimean EQs with magnitude approximately 4 [27] and 2 months for Tohoku EQ with magnitude 9 according to our study.

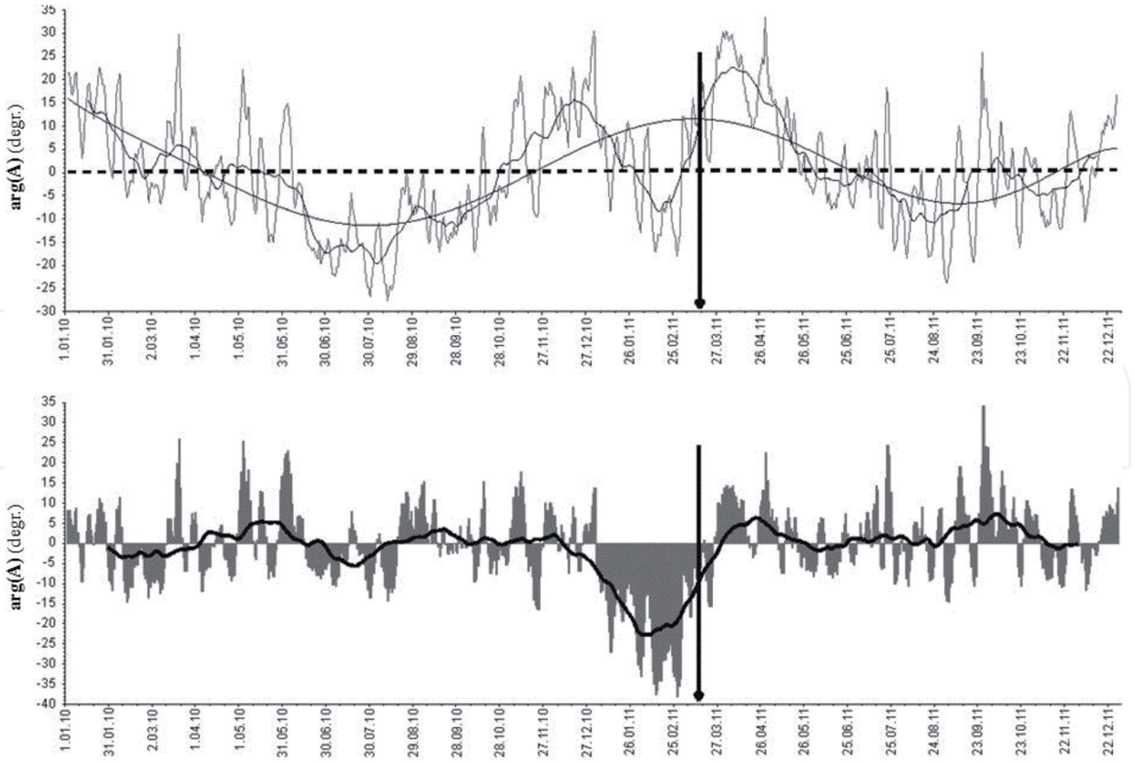

Figure 8.
*Variations of arg(*A*) for the period T = 100 s at the observatory KNZ by the data for 2010–2011 years. (a) Rough gray curve is the result of everyday processing after moving averaging with window length of 5 days with 1-day shift. Bold solid line is the result of averaging with moving window of 29 days (for elimination of monthly variation) with 1-day shift. (The first -, second-, and seventh (quasi-annual)-order polynomials determined from seven years data and presented in* ***Figure 7a*** *were subtracted). The time of the Tohoku EQ on 11.03.2011 is marked by a vertical arrow. (b) The same after the removal of residual annual variation determined from 2010-2011 data and given in* ***Figure 8(a)*** *by thin line.*

Kopytenko et al. [24] compared nighttime records of KAK and UCU observatories (see **Figures 3**, **6**) in frequency range of 0.33–0.01 Hz for the interval of 21 days before the Tohoku EQ, that is, since February 2, 2011 till March 3, 2011. They found the appearance of anomalous changes on February 22, 2011 (18 days before EQ): decrease of the correlation coefficients between geomagnetic components of KAK and UCU observatories and rise of B_z component in sub-diapason 0.033–0.01 Hz. It was interpreted as appearance LE.

Now let us see **Figure 5b**. It presents nighttime records on February 24, 2011, 16 days before the Tohoku EQ, in geomagnetically quite interval with rather good temporal and amplitude resolution. MT variations in the horizontal components are almost the same at all presented observatories distributed at the territory 2000 km long. In the records of UCU and KNZ (separated by 17 km) we see strong varitations with frequencies of 0.002–0.1 Hz and amplitude of 0.2 and 0.5 nT, respectively, and even more strong variations in B_z component. All of this is in good agreement with the results of [24]. Variations in KNZ and UCU cover approximately the same frequency diapason as in [24], slightly correlate one with the other, and are not observed at other observatories. All signs of LE! But we cannot exclude that there are some remainders of the daytime noise from DC traffic. We need several more observatories (as SES network in Greece) for more definite conclusions.

5. Discussion of LE features

To use the LE for EQ prediction, one needs to know its lead time, amplitude, frequency characteristic, and expected distribution of sensitive places in the Earth

Earthquake	Δr, km	Δt, day or hour	A, nT	f, Hz	A/Δr, nT/km
Alaska M9.2	440 (30)	1 h	100		0.28 (3.3)
Loma Prieta M7.1	7	36 day, 13 day, 3–0 h	1.5, 2, 5	0.01–0.5	0.21 0.29 0.71
Taiwan Chi-Chi M7.6	80 (≈5)	>32 day, 10–2 days	200		2.5 (40)
Spitak M6.9	130	4 h	0.1	0.1–1	0.001
Racha aftershock M6.2	≈50	4–1 days, few h	≈1	0.1–1	0.02
Racha aftershock M4	35	Hours	1	0.1–1	0.029
Greneva-Kozani M6.6	80	25 days	≈1?	≈0.05?	

Δr, distance between observatory and EQ epicenter (or nearby displacement fault, given in brackets); Δt, lead time of LE appearance before the EQ; A, LE amplitude; f, frequencies at which LE was recorded or the maximum of LE frequency characteristic. Scatter of A/Δr ratio shows strong irregularities in spatial decay of LE.

Table 2.
Parameters of the observed LE.

surface. This knowledge can be obtained now only empirically. We can extract the necessary properties from the data presented in Section 1.3 supplementing them with other published data. An attempt of such extraction is presented in **Table 2**.

The results depend of the conditions of observation. So, sampling rate of 10 min and compressed time scale in [12] describing two EQs in Taiwan exclude frequency content estimation. Important parameter – lead time Δt is properly determined only before Loma Prieta EQ when signal-to-noise ratio was large during long time that allowed separate three stages of the precursor appearance. Spatial selectivity complicates the formulation of the LE spatial regularities. Thus, we are in the very beginning of LE phenomenon study and use.

6. Conclusions

We have calculated induction vectors using data from Japanese observatories for many years preceding the 2011 Tohoku EQ. In 2008–2010 at six observatories, we found anomalous variations of induction vectors, which are regarded as middle-term EQ precursors. Those observatories are located not at the shortest distances from the EQ epicenter, which is in general agreement with the well-known phenomenon of spatial selectivity of EQ precursors. The analysis of horizontal tensors reveals a conductivity anomaly under the central part of the Boso peninsula with a WNW-ESE strike coinciding both with the Sagami trough strike and well conducting 3-km-thick sediment strike. A joint analysis of geoelectric and tectonic data leads to a preliminary conclusion that the Boso conductivity anomaly connects two large-scale conductors: Pacific seawater and a deep magma reservoir beneath a volcanic belt. Similar anomaly was found earlier in Kamchatka [21]. Then, applying original data analysis with the elimination of annual and monthly variations, we separated two-month-long short-term EQ precursor of the Tohoku EQ.

Several cases of lithosphere emission LE before strong EQs were reviewed and analyzed, and preliminary portrait of LE precursor was compiled: LE can appear several times with lead time a month(s), weeks, days, hours, and minutes and can attain amplitude several hundreds of nT which rapidly and not uniformly diminishes with moving away from the source. Typical frequency content/maximum is 0.01–0.5 Hz. As it is widely accepted [5], LE is generated by the process of

microcracks opening in the course of EQ preparation and should be a rather common phenomenon. It is not quite clear how high-frequency microcrack radiation propagates through many kilometers of the Earth's crust to be recorded at the Earth surface. Seemingly, the radiation finds the optimal pathways leading to sensitive places on the earth surface where signal can be observed. Then, the search of sensitive spots opens new channel of information for the Earth interior study.

Recommendation on the LE monitoring for the strong EQ prediction

1. Network must allow the gradient measurements, so a minimum of three magnetometers must be installed for synchronous records [24].

2. The best but very expensive is the SES monitoring network in Greece. Electrical dipoles can be supplemented or replaced by magnetometers. We recommended for use the practice of sensitive places search and use [11] and the methodology of LE sophisticated analysis developing by Prof. Varotsos' team [14, 15].

3. RF approach is a valuable supplement to LE. It has lower temporal resolution but yields additional information on the conductivity variations in the EQ preparation zone.

Author details

Igor I. Rokityansky*, Valeriia I. Babak and Artem V. Tereshyn
Ukrainian National Academy of Sciences, Subbotin Institute of Geophysics, Kiev, Ukraine

*Address all correspondence to: rokityansky@gmail.com

References

[1] Wang K, Chen Q-F, Sun S, Wang A. Predicting the 1975 Haicheng earthquake. Bulletin of the Seismological Society of America. June 2006;**96**(3): 757-795. DOI: 10.1785/0120050191

[2] Rokityansky II. Geoelectromagnetic Investigation of the Earth's Crust and Mantle. Berlin Heidelberg New York: Springer-Verlag; 1982. 381 p

[3] Berdichevsky MN, Dmitriev VI. Models and Methods of Magnetotellurics. Berlin Heidelberg: Springer-Verlag; 2008. 564 p. DOI: 10.1007/978-3-540-77814-1

[4] Chave AD, Jones AG, editors. The Magnetotelluric Method. Cambridge: Cambridge University Press; 2012. 584 p. DOI: 10.1017/CBO9781139020138.002

[5] Surkov V, Hayakawa M. Ultra and Extremely Low Frequency Electromagnetic Fields. London: Springer Geophysics; 2014. 486 p. DOI: 10.1007/978-4-431-54367-1

[6] Moore GW. Magnetic disturbances preceding the 1964 Alaska earthquake. Nature. 1964;**203**:508-509. DOI: 10.1038/203508b0

[7] Frather-Smith AC, Bernardi A, McGill PR, Ladd ME, Helliwell RA, Villard OG Jr. Low-frequency magnetic field measurements near the epicenter of the Ms 7.1 Loma Prieta earthquake. Geophysical Research Letters. 1990;**17**(9):1465-1468. DOI: 10.1029/GL017i009p01465

[8] Kopytenko YA, Matiashvili TG, Voronov PM, Kopytenko EA, Molchanov OA. Detection of ultra-low-frequency emissions connected with Spitak earthquake and its aftershock activity, based on geomagnetic pulsations data at Dusheti and Vardzia observatories. Physics of the Earth and Planetary Interiors. 1993;**77**:85-95

[9] Kopytenko YA, Matiashvili TG, Voronov PM, Kopytenko EA. Observation of electromagnetic ultralow-frequency lithospheric emission in the Caucasian seismically active zone and their connection with earthquakes. In: Hayakawa b M, Fujinawa Y, editors. Electromagnetic Phenomena Related to Earthquake Prediction. Tokyo: Terra Scientific Publishing Company (TERRAPUB); 1994. pp. 175-180

[10] Rokityansky II. Spatial selectivity of earthquake's precursors. Physics and Chemistry of the Earth. 2006;**31**: 204-209. DOI: doi.org/10.1016/j.pce.2006.02.028

[11] Varotsos AP. The Physics of Seismic Electric Signals. Tokyo, Japan: TERRAPUB; 2005. 338 p

[12] Tsai YB, Liu JY, Ma KF, Yen HY, Chen KS, Chen YI, et al. Precursory phenomena associated with the 1999 chi-chi earthquake in Taiwan as identified under the ISTEP program. Physics and Chemistry of the Earth. 2006;**31**:365-377

[13] Varotsos P, Alexopoulos K, Lazaridou M. Latest aspects of earthquake prediction in Greece based on seismic electric signals, II. Tectonophysics. 1993;**224**:1-37. DOI: 10.1016/0040-1951(93)90055-O

[14] Varotsos PA, Sarlis NV, Skordas ES, Lazaridou MS. Seismic electric signals: An additional fact showing their physical interconnection with seismicity. Tectonophysics. 2013;**589**:116-125. DOI: 10.1016/j.tecto.2012.12.020

[15] Sarlis NV, Skordas ES, Varotsos PA, Nagao T, Kamogawa M, Tanaka H, et al. Minimum of the order parameter fluctuations of seismicity before major earthquakes in Japan. Proceedings of the National Academy of Sciences of the United States of America.

2013;**110**:13734-13738. DOI: 10.1073/pnas.1312740110

[16] Yanagihara K, Nagano T. Time changes of transfer function in the Central Japan anomaly of conductivity with special reference to earthquake occurrences. Journal of Geomagnetism and Geoelectricity. 1976;**28**(2):157-163

[17] Fujita S. Monitoring of time changes of conductivity anomaly transfer functions at Japanese magnetic observatory network. Memoirs of the Kakioka Magnetic Observatory. 1990;**23**:53-87

[18] Fujiwara S. Temporal changes of geomagnetic transfer functions using data obtained mainly by the geographical survey institute. Bull Bulletin of the Geographical Survey Institute. 1996;**41**:1-25

[19] Rokityansky II, Tregubenko VI, Babak VI, Tereshyn AV. Induction vector and horizontal tensor components variations before the Tohoku earthquake on the 11th march 2011 according to the data of Japanese geomagnetic observatories. Geophysical Journal. 2013;**35**(3):115-130. (in Russian)

[20] Rokityansky II, Babak VI, Tereshyn AV. Geomagnetic activity impacts on the results of the induction vector calculations. Geophysical Journal. 2015;**37**(6):86-98. (in Russian)

[21] Rokityansky II, Babak VI, Tereshyn AV. An analysis of geomagnetic response functions prior to the Tohoku, Japan earthquake. Journal of Volcanology and Seismology. 2016;**10**(6):78-91

[22] Varentsov IM. Arrays of simultaneous EM soundings: Design, data processing and analysis. In: Spichak V, editor. EM Sounding of the Earth's Interior. Methods in Geochemistry and Geophysics. Vol. 40. Heidelberg, London: Elsevier; 2007. pp. 259-275. DOI: 10.1016/S0076-6895(06)40010-X

[23] Klymkovych TA. Peculiarities of temporal variations of anomalous magnetic field and induction vectors in the Transcarpathian seismic-active trough [PhD thesis] Kiev: Institute of Geophysics; 2009 (in Ukrainian)

[24] Kopytenko YA, Ismaguilov VS, Hattori K, Hayakawa M. Anomaly disturbances of the magnetic fields before the strong earthquake in Japan on march 11, 2011. Annals of Geophysics (Italy). 2012;**55**(1):101-107. DOI: 10.4401/ag-5260

[25] Suzuki H. Underground geological structure beneath the Kanto plain, Japan. National Research Institute for Earth Science and Disaster Prevention, Japan. 2002;**63**:1-19

[26] Takahashi M, Yanagisawa Y, Hayashi H, Kasahara K, Ikawa T, Kawanaka T, et al. Miocene subsurface half-grabens in the Kanto plain, Central Japan. Proceeding of International Workshop on Strong Ground Motion Prediction and Earthquake Tectonics in Urban Areas. 2005:65-74

[27] Tregubenko VI. Seismoprognostic researches. In: Goshovsky SV, editor. 50 Years of Ukrainian State Geological Institute (1957-2007). Anniversary Directory. Kyiv: Ukr SGPI; 2007. pp. 52-56 (in Ukrainian)